Robust Gust Load Alleviation for a Flexible Aircraft

N. Aouf * B. Boulet * R.M. Botez **

ABSTRACT

An H_∞ controller design is presented to establish a nominal performance baseline for the vertical acceleration control of a B-52 aircraft model with flexibility. The technique of μ-synthesis and analysis is used to study the robust performance of the aircraft taking into account specific input and output multiplicative uncertainty models. The aircraft is assumed to be subjected to severe wind gusts causing undesirable vertical motion. We use the Dryden gust power spectral density model to guide the performance specifications and control designs, as well as for time-domain simulations. Motivation for the use of an H_∞ nominal performance baseline specification is given in terms of a new interpretation of the Dryden model. The H_∞ optimal controller is shown to reduce dramatically the effect of wind gust on the aircraft vertical acceleration. Robust performance is achieved with a μ-synthesis controller design using a D-K iteration procedure.

RÉSUMÉ

Un régulateur H_∞ est présenté afin d'établir une performance nominale de base pour la commande d'accélération verticale d'un modèle d'avion flexible, soit le bombardier B-52. La technique de synthèse et d'analyse μ est utilisée pour l'étude de la performance robuste de l'avion, prenant compte des modèles d'incertitudes multiplicatives à l'entrée et à la sortie du modèle. On suppose que le bombardier est soumis à une violente rafale produisant un mouvement vertical indésirable. Nous utilisons le modèle de Dryden pour la densité spectrale de puissance de la rafale afin d'établir des spécifications de performance dans notre méthode de conception, ainsi que dans des simulations temporelles. L'utilisation de spécifications de performance nominale dans H_∞ est justifiée en termes d'une réinterprétation du modèle de Dryden. On montre que le régulateur optimal H_∞ réduit grandement l'effet de la rafale sur l'accélération verticale de l'avion. La performance robuste est atteinte à l'aide d'un régulateur de synthèse μ obtenu par une itération D-K.

*Centre for Intelligent Machines
McGill University, 3480 University Street,
Montréal, Québec Canada H3A 2A7
**Département de Génie de la production automatisée
Ecole de technologie supérieure
1100 Notre-Dame Street West,
Montréal, Québec, Canada H3C 1K3

INTRODUCTION

Gust load alleviation (GLA) systems can be used to reduce the effects of wind gusts on vertical acceleration of aircraft. Their purpose is to reduce airframe loads and improve passenger comfort. In this paper, the longitudinal dynamics of the B-52 bomber are studied (Mclean, 1990). The dynamic model of the aircraft includes structural flexibility. Such a model is more realistic than a rigid-body model, but it can also make feedback control design for gust load alleviation more challenging.

We present H_∞ and μ controller designs for a model of the B-52 aircraft with flexible modes. The gust is generated with the Dryden power spectral density model. This kind of model lends itself well to frequency-domain performance specifications in the form weighting functions. The H_∞ and μ controllers are shown to meet the desired nominal performance and the robust performance specifications with reasonably small control surface deflection angles. Previous research on GLA control systems reported in References 3, 5 and 7 take approaches different to ours, notably LQG and H_∞ for a rigid-body aircraft.

GUST MODEL

Two classical analytical representations for the power spectral density (PSD) function of atmospheric turbulence were given by Von Kármán and Dryden (Mclean, 1990). As the Dryden PSD function has a simpler form than Von Kármán's, we chose to use the former. It can be written as:

$$\Phi_w(\omega) = \frac{\sigma_w^2 L_w \left[1 + 3\left(\frac{L_w \omega}{U_0}\right)^2\right]}{\pi U_0 \left[1 + \left(\frac{L_w \omega}{U_0}\right)^2\right]^2} \tag{1}$$

where:

σ_w is the RMS vertical gust velocity (*m/s*),
L_w is the scale of turbulence (*m*), and
U_o is the aircraft trim velocity (*m/s*).

The scale length L_w is dependent on the aircraft's height h when atmospheric turbulence is encountered, as follows:

At $h > 580$ m (1750 ft), $L_w = 580$ m,
At $h < 580$ m, $L_w = h$ m.

For thunderstorms, at any height:
$L_w = 580$ m (1750 ft), $\sigma_w = 7$ m/s (21 ft/s).

Gust signals have to be generated with the required intensity, scale lengths and PSD functions for some given flight velocity and height. In order to generate these gust signals, a noise source with PSD function $\Phi_n(\omega) = 1$ in the frequency band of interest is used to provide the input signal to a linear filter $G_w(s)$ chosen such that the squared magnitude of its frequency response is the PSD function $\Phi_n(\omega)$. The gust generator setup is as follows:

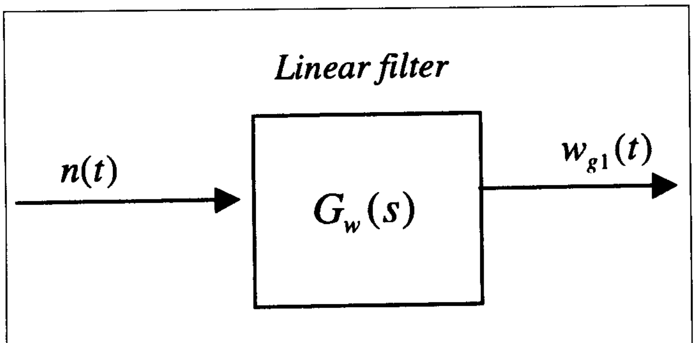

Figure 1.
Gust signal generator.

where $n(t) \sim N(0,1)$ is a Gaussian white noise process of unit intensity and zero mean, and $w_{g1}(t)$ is the random continuous vertical gust, so that, formally, $w_{g1}(t) = G_w n$. The PSD of the output signal is related to the PSD of the input signal as follows:

$$\Phi_w(\omega) = |G_w(j\omega)|^2 \, \Phi_n(\omega) = |G_w(j\omega)|^2 \quad . \tag{2}$$

An expression for the Dryden filter can be found through spectral factorization of $\Phi_w(\omega)$, which yields

$$G_w(s) = \sqrt{\frac{3U_0\sigma^2_w}{\pi L_w}} \; \frac{\dfrac{U_0}{\sqrt{3}L_w} + s}{\left[\dfrac{U_0}{L_w} + s\right]^2} \quad . \tag{3}$$

A proposed alternative use of the Dryden model is to consider the noise n to be any deterministic finite-energy signal in $\mathcal{N} := \{n \in \mathcal{L}_2[0,\infty) : \|n\|_2 \le 1\}$. The gust signal lives in $\mathcal{W} = \{G_w n : n \in \mathcal{N}\} \subset \mathcal{L}_2[0,\infty)$ and its energy is bounded by

$$\|w_g\|_2^2 \le \|G_w\|_\infty^2 = \frac{81\sigma_w^2 L_w}{50\pi U_0} \quad .$$

Furthermore, such signals taper off at infinity in the time domain. Hence, they may be more representative of real wind gusts acting on an aircraft passing through a turbulence. Although the stochastic nature of the signal is lost, the resulting set of bounded-energy gust signals can be used for a worst-case H_∞ design, which is desirable in a safety-critical application such as GLA.

Flexible Aircraft Model

The short-period approximation for the rigid-body motion of the B-52 aircraft is considered. The aircraft's rigid-body dynamics equations are augmented by adding to the state variables a set of generalized coordinates associated with the normal bending modes. Structural displacement was considered small compared to the whole aircraft structure. The j^{th} flexible mode is represented by the following second-order linear constant-coefficient differential equation in terms of its modal coordinate η_j:

$$\ddot{\eta}_j + 2\zeta_j\omega_j\dot{\eta}_j + \omega_j^2\eta_j = \rho_j\phi_j \tag{4}$$

where ζ_j, ω_j, ρ_j are the damping ratio, frequency and gain of the j^{th} flexible mode, and ϕ_j is its corresponding generalized force. Thus, the rigid aircraft dynamics may be augmented with pairs of first-order equations corresponding to each flexible mode considered. Five structural flexible modes were considered significant and were kept in the longitudinal dynamic model of the B-52 aircraft (Mclean, 1978).

The control inputs for the longitudinal motion are the deflection angles (in radians) of the elevator δ_{el} and the horizontal canard δ_{hc}. The longitudinal dynamics of the flexible aircraft in terms of the state variable representation is:

$$\begin{aligned} \dot{x}(t) &= Ax(t) + Bu(t) + B_g w_g(t) \\ y(t) &= Cx(t) + Du(t) \end{aligned} \tag{5}$$

where $x(t) \in \mathbb{R}^{12}$ is the state vector :
$x^T = [\alpha \;\; q \;\; \eta_1 \;\; \dot{\eta}_1 \;\; \eta_5 \;\; \dot{\eta}_5 \;\; \eta_7 \;\; \dot{\eta}_7 \;\; \eta_8 \;\; \dot{\eta}_8 \;\; \eta_{12} \;\; \dot{\eta}_{12}]$, $u(t) \in \mathbb{R}^2$ is the control vector: $u = [\delta_{el} \;\; \delta_{hc}]^T$ (radians), $y(t) \in \mathbb{R}$ is the vertical acceleration (g), $w_g(t) \in \mathbb{R}^3$ is the vertical gust velocity at three stations (m/s) , $\alpha(t) \in \mathbb{R}$ is the angle of attack (radians) and $q(t) \in \mathbb{R}$ is the pitch rate (radians/s).

The form of the A matrix in state-space Equation 5 shows the couplings between the aircraft's flexible structure and rigid-body dynamics:

$$A = \begin{bmatrix} A_{rr} & A_{ra} \\ A_{ar} & A_{aa} \end{bmatrix} \tag{6}$$

where A_{rr} are the rigid-body terms, A_{ra} the rigid/aeroelastic terms, A_{ar} the aeroelastic/rigid terms, and A_{aa} the structural flexibility terms. The two eigenvalues of A corresponding to the rigid-body mode are $\lambda_{1,2} = -1.803 \pm j\, 2.617$. The five flexible modes are listed in **Table 1**.

Table 1. Flexible modes.					
Mode no.	1	2	3	4	5
ω_i (rd/s)	7.60	15.22	19.73	20.24	38.29
ζ_i	0.393	0.056	0.011	0.067	0.023

Input terms associated with the effects of wind gust acting at three different body stations are also included in Equation 5. They appear as three different gust signals w_{g1}, w_{g2}, and w_{g3} acting in the longitudinal dynamic equations. Thus, the gust vector is defined as $w_g = [w_{g1}\ w_{g2}\ w_{g3}]^T$.

The second and third gust signals w_{g2} and w_{g3} are time-delayed versions of w_{g1}. The second gust is delayed by a time $\tau_1 = U_0/x_1 = 0.06$ s, where x_1 is the distance from the first body station, which encounters the gust first. The third input is delayed by time $\tau_2 = U_0/x_2 = 0.145$ s. First-order lags are used to model the delays for simplicity, but Padé approximations could be used as well. The formal generation of the gust vector is shown in **Figure 2**.

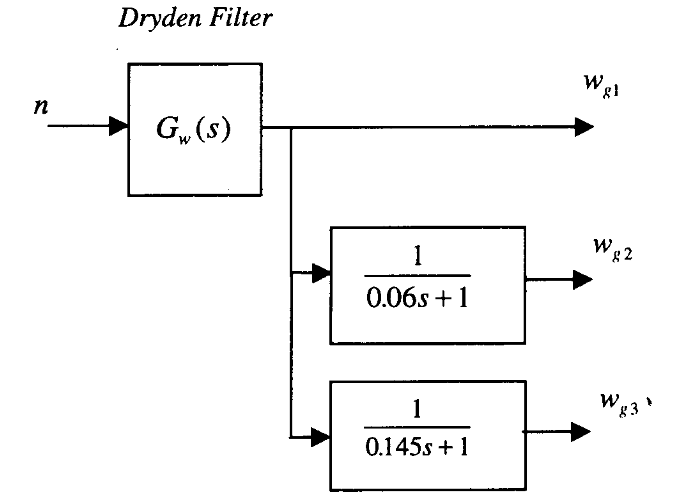

Figure 2.
Gust signals at three body stations.

The signal w_{n1} is a small disturbance that has a role to play in regularizing the H_∞ design problem. It can also be seen as a real measurement noise. Its amplitude is specified by $\epsilon = 10^{-4}$ as w_n is assumed to have a maximum amplitude of 1. For convenience, we will use the notation $T_{xy} := x \mapsto y$ for closed-loop transfer matrices mapping signal x to signal y.

H_∞ - Optimal Control

Problem Setup

A block diagram of the closed-loop gust alleviation design problem with weighting functions is shown in **Figure 3** below: where $w_g(t)\in\mathbb{R}^3$ is the gust disturbance, $w_{n1}(t)\in\mathbb{R}$ is an acceleration measurement noise, $r = 0$ is the vertical acceleration setpoint, $z_1(t)\in\mathbb{R}$ is the weighted measured error, and $z_2(t)\in\mathbb{R}^2$ is the weighted controller output. The plant transfer matrix $G(s)$ mapping $[u\ w_g^T]^T$ to y is given by:

$$G(s) = \left[\begin{array}{c|c} A & [B\ B_g] \\ \hline C & [D\ 0] \end{array}\right] \qquad (7)$$

Weighting Functions for Nominal Performance

Choosing $\sigma_w = 7m/s$, $L_w = 580m$ in the Dryden model, we obtain a gust that has most of its power concentrated in the frequency band [0.1, 6] Hz. The specification is that our controller has to be able to regulate the vertical acceleration in this interval with an amplitude attenuation of at least 500 (-54 dB).

The closed-loop vertical acceleration of the aircraft can be written in terms of the gust vector w_g and the disturbance w_n as follows:

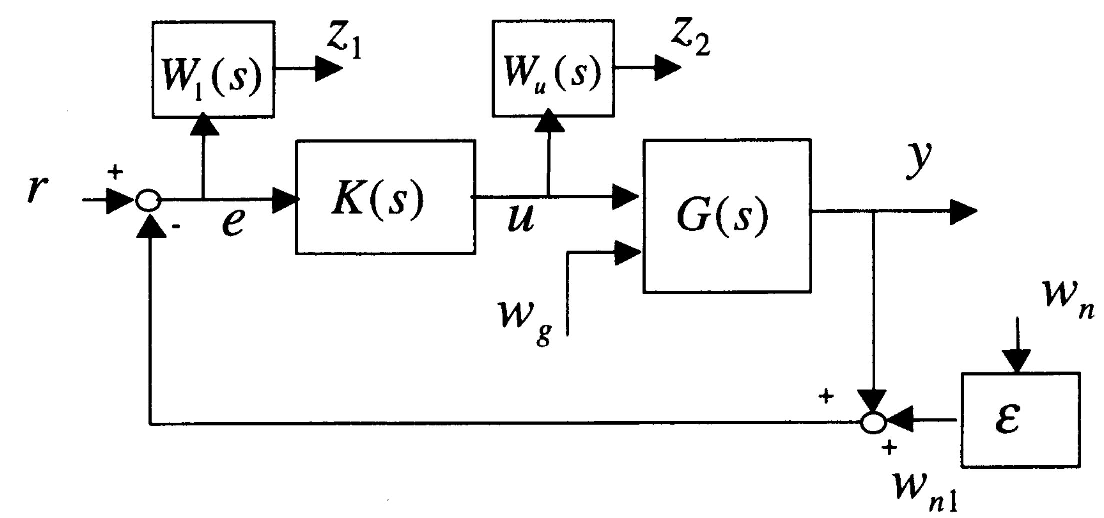

Figure 3.
Setup for H_∞ control.

$$y = T_{w_g y} w_g + T_{w_n y} w_n \tag{8}$$

where $T_{w_g y}$ and $T_{w_n y}$ are the transfer matrices mapping w_g and w_n to y respectively. Thus, the controller has to minimize $||T_{w_g y}(j\omega)||$ and $||T_{w_n y}(j\omega)||$ over [0.1,6] Hz. The gust alleviation performance specification on $||T_{w_g y}(j\omega)||$ can be enforced through the use of a weighting function $W_1(s)$ of amplitude at least 500 over [0.1, 6]Hz , as long as we get $||W_1 T_{w_g y}||_\infty$ with the controller K, which implies

$$|| T_{w_g y}(j\omega) || < | W_w(j\omega) |^{-1} \quad . \tag{9}$$

The weighting function is

$$W_1(s) = \frac{k_1}{a_0 s + 1} \tag{10}$$

with k_1 = 500, a_0 = 0.05. A plot of $|W_1(j\omega)|^{-1}$ is shown in **Figure 5**.

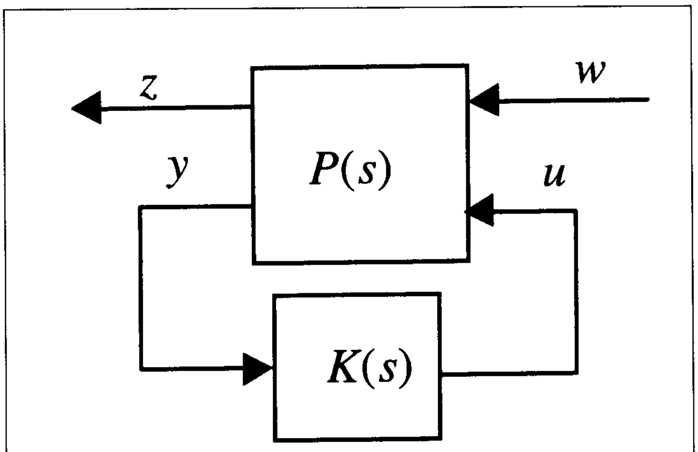

Figure 4.
Standard setup for H_∞ control.

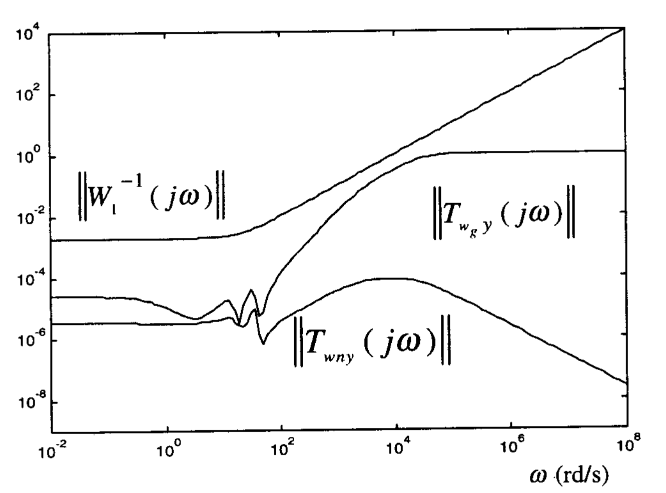

Figure 5.
Achieved performance.

The controller outputs consist of deflection angles (in radians) of the aircraft's elevators and horizontal canards. In order to make sure that these angles will remain within acceptable limits, we took the output of the controller u as one of the controlled variable z_2. Define the input vector w: = $[w_g^T \; w_n]^T$. The use of a suitable weighting function W_u on u such that $||W_u T_{wu}||_\infty < 1$ in closed loop minimizes actuator travel while meeting the other performance specification. The weighting function W_u is a diagonal transfer matrix

$$\begin{bmatrix} W_{u1} & 0 \\ 0 & W_{u2} \end{bmatrix}$$

so that the above H_∞-norm condition implies

$$|| T_{wu1}(j\omega) || < | W_{u1}(j\omega) |^{-1} \tag{11}$$

and

$$|| T_{wu2}(j\omega) || < | W_{u2}(j\omega) |^{-1} \tag{12}$$

where

$$T_{wu} = \begin{bmatrix} T_{wu1} \\ T_{wu2} \end{bmatrix} .$$

In our study, we tried two different types of control weighting functions. The first type is composed of two first-order biproper filters

$$W_u^1(s) = \begin{bmatrix} \dfrac{s + \omega_{c1} / l_{u1}}{\epsilon_1 s + \omega_{c1}} & 0 \\ 0 & \dfrac{s + \omega_{c2} / l_{u2}}{\epsilon_2 s + \omega_{c2}} \end{bmatrix} \tag{13}$$

where ϵ_1, ϵ_2 are very small. The parameters l_{u1} and l_{u2} represent the maximum controller gains at frequencies below the cutoff frequencies ω_{c1} and ω_{c2}. The second type of control weighting function that we tried is constant:

$$W_u^2 = \begin{bmatrix} k_{u1} & 0 \\ 0 & k_{u2} \end{bmatrix} \quad . \tag{14}$$

Here $1/k_{u1}$ and $1/k_{u2}$ represent the maximum controller gains at all frequencies in closed loop. For both types of weighting functions, we took $k_{u1}^{-1} = l_{u1} = 0.2$, $k_{u2}^{-1} = l_{u2} = 0.5$ and $\epsilon_1 = \epsilon_2 = 0.0001$.

The weighting function $W_u^1(s)$ gives us more degrees of freedom to constrain the control signals in order to satisfy physical actuator saturation and bandwidth constraints. In our case study, the filter cutoff frequencies were selected as ω_{c1} = 12, ω_{c2} = 13 rd/s. However, it finally proved preferable to use the constant weighting matrix W_u^2 for our application, since it did not increase the order of the generalized plant model P(s) by 2 like $W_u^1(s)$ would, (hence the resulting H_∞ controller would have a lower order). Moreover, the resulting closed-loop transfer functions still satisfied inequalities (Equation 11 and Equation 12) with $W_u^1(s)$. **Figures 6** and **7** show the magnitude of W_u with both forms.

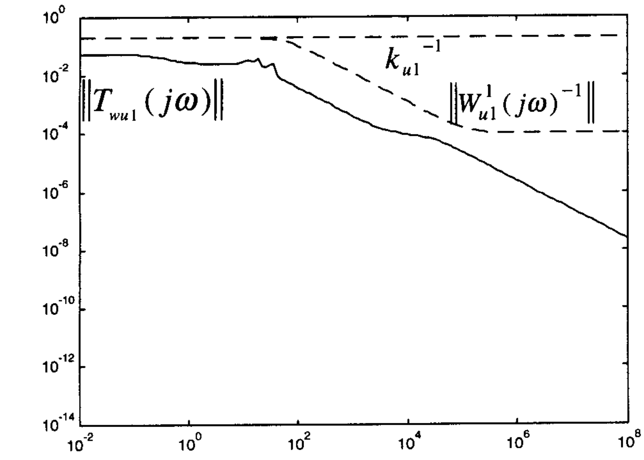

Figure 6.
Constraint on elevator angle.

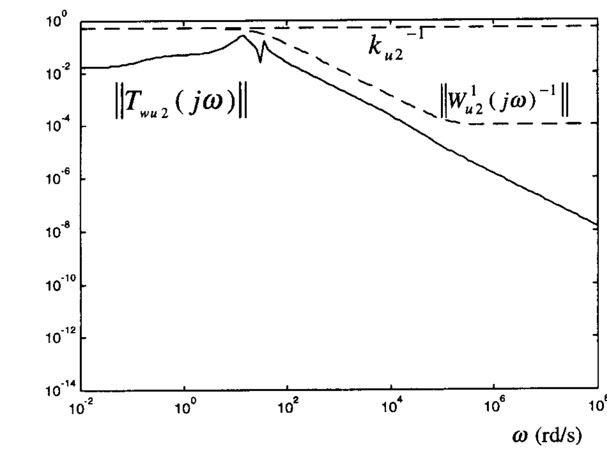

Figure 7.
Constraint on horizontal canard angle.

H_∞ Controller

The GLA problem of **Figure 3** can be recast into the standard H_∞-optimal control problem (Doyle *et al.*, 1988) of **Figure 4**.

The nominal generalized plant model

$$P(s)=\begin{bmatrix} P_{11}(s) & P_{12}(s) \\ P_{21}(s) & P_{22}(s) \end{bmatrix} \tag{15}$$

has a minimal state-space realization

$$\begin{aligned} \dot{x} &= A_p x + B_{P1} w + B_{P2} u \\ z &= C_{P1} x + D_{P11} w + D_{P12} u \\ y &= C_{P2} x + D_{P21} w + D_{P22} u \end{aligned} \tag{16}$$

which combines the aircraft model and realizations of the weighting functions. The vector of exogenous signals is $w = [w_g^T\ w_n]^T$ and the signals to be minimized are collected in $z:=[y\ u^T]^T$.

As gusts act over a relatively short period of time, they can be considered as signals with finite energy. Such signals can have spectral contents similar to the *PSD* of stochastic Dryden gust signals by using $G_w(s)$ as a filter. This remark provides motivation for H_∞ GLA control design, as

$$\begin{aligned} &\min_{K\in S}\max_{w\in W}\|T_{wz}w\|_2 = \min_{K\in S}\max_{n\in N}\|T_{wz}G_w n\|_2 \\ &= \min_{K\in S}\|T_{wz}G_w\|_\infty = \min_{K\in S}\sup_{\omega\in\mathbb{R}}\|T_{wz}(j\omega)G_w(j\omega)\| \end{aligned} \tag{17}$$

where S is the set of all finite-dimensional, causal linear time-invariant stabilizing controllers. Note that we chose to use the performance weighting function $W_1(s)$ instead of $G_w(s)$ in our design, but $|W_1(j\omega)|>|G_w(j\omega)|$ at all frequencies, which leads to better performance.

The overall objective in this H_∞-optimal controller design was to minimize $\|T_{wz}\|_\infty$ over the set S, in order to get $\|T_{wz}\|_\infty < 1$. This would guarantee that the performance specification is satisfied on the nominal model. Following Reference 4, an H_∞ controller $K(s)$ of order 13 was designed using the Matlab μ-Analysis and Synthesis Toolbox (Balas *et al.*, 1995) that achieved a norm of $\|T_{wz}\|_\infty = 0.68$. **Figure 5** shows that our H_∞ controller meets the gust alleviation performance specification given above. We can see that the maximum singular value of $T_{w_g y}$ is well below 10^{-4} over $2\pi[0.1,6]$ rd/s.

The norms (maximum singular values) of the frequency responses of T_{wu1} and T_{wu2} shown in **Figures 6** and **7** satisfy the constraints of Equation 11 and Equation 12 for both control weighting functions as mentioned above.

μ - Controller

The H_∞ controller design of the previous section provides nominal performance. That is, performance is guaranteed only if the model represents the aircraft's dynamics perfectly, which is clearly too optimistic. In this section, uncertainty in the frequency responses of the actuators and sensors is taken into account in the model and the controller design. Note that this uncertainty may also include variations in the aerodynamics of the control surfaces which may be caused by changes in altitude and velocity of the aircraft. As shown in **Figure 8**, we include two complex multiplicative uncertainty blocks in the model: $\Delta_u := \text{diag}\{\Delta_{u1}, \Delta_{u2}\}$, $\Delta_{u1}, \Delta_{u2} \in \mathbb{C}$ and $\Delta_y \in \mathbb{C}$. These perturbations represent the uncertainty in the frequency responses of the actuators and the sensor, respectively. We chose the corresponding weighting functions to be:

$$W_{uncu} = \begin{bmatrix} \dfrac{0.75s+50}{s+400} & 0 \\ 0 & \dfrac{0.75s+22.5}{s+400} \end{bmatrix} \tag{18}$$

$$W_{uncy} = \frac{0.15s+30}{s+1000} \quad . \tag{19}$$

These weighting functions are selected such that the magnitudes of their frequency responses represent the maximum error (away from unity) in the actuators and sensor models at each frequency. Typically, multiplicative perturbations are small at low frequencies and rise toward or above one at high frequencies. The weighting functions can be obtained by finding an upper bound on several Bode plots of possible perturbations. For example, suppose that an uncertain, parameterized model $G_s(p,s)$ of the sensor is available, where p is the vector of parameters with known bounds. Then, one can fit a weighting function $W_{uncy}(j\omega)$ such that its magnitude is a tight upper bound of all the plots of $|G_s(p_i, j\omega) - 1|$ for i = 1, ..., M, where p_i is a set of parameters within their bounds. The weighting functions can also be obtained from experimental frequency-response input-output data.

One must keep in mind that these weights represent the size of the uncertainty and should thus be seen as hard constraints, not design parameters. It is the performance weighting functions that may be changed until a good robustness/performance tradeoff is obtained in the design.

The block diagram of **Figure 8** can be recast into the general μ-synthesis setup as given by **Figure 9**. Define the complex structured uncertainty set

$$\Omega := \{\Delta = \text{blockdiag}\{\Delta_{u1}, \Delta_{u2}, \Delta_y\} : \Delta_{u1}, \Delta_{u2}, \Delta_y \in \mathbb{C}\} \subset \mathbb{C}^{3\times3} \tag{20}$$

and the augmented structured uncertainty set

$$\Gamma := \{\Delta_s = \text{blockdiag}\{\Delta, \Delta_p\} : \Delta \in \Omega, \Delta_p \in \mathbb{C}^{4\times3}\} \subset \mathbb{C}^{7\times6} \tag{21}$$

where $\Delta_p \in \mathbb{C}^{4\times3}$ is a fictitious uncertainty linking the exogenous inputs $[w_g \;\; w_n]^T$ to the output variables $[z_1 \;\; z_2]^T$. This fictitious perturbation is included to transform a robust performance design problem into an equivalent robust stability problem, which is easier to solve (Balas *et al.*, 1995). The inputs and

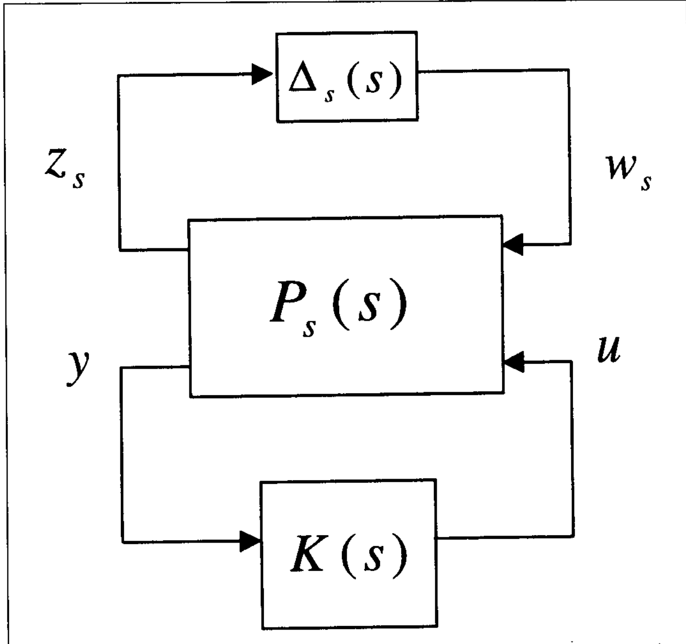

Figure 9.
Standard setup for μ design.

outputs of the structured uncertainty $\Delta_s(s) \in H_\infty$, $\Delta_s(j\omega) \in \Gamma$ in **Figure 9** are, respectively, the vectors $z_s = [z_3^T \, z_4 \, z_1 \, z_2^T]^T \in \mathbb{R}^6$ and $w_s = [w_3^T \, w_4 \, w_g^T \, w_n]^T \in \mathbb{R}^7$.

The structured singular value μ_Γ of a complex matrix $M \in \mathbb{C}^{6\times7}$ is defined with respect to the structured uncertainty set Γ as follows:

$$\mu_\Gamma(M) := \min\{\|\Delta\| : \Delta \in \Gamma, \det(I - M\Delta) = 0\}^{-1} \tag{22}$$

unless no such perturbation exists, in which case $\mu_\Gamma(M) = 0$.

A robust controller design based on μ_Γ is less conservative than a robust H_∞ design (not to be confused with our H_∞ controller of the previous section which is optimal for the nominal model, but was not designed to be robust to model uncertainty). This is because the structured uncertainty Δ_s is taken into account as a full block of uncertainty in a typical robust H_∞ design.

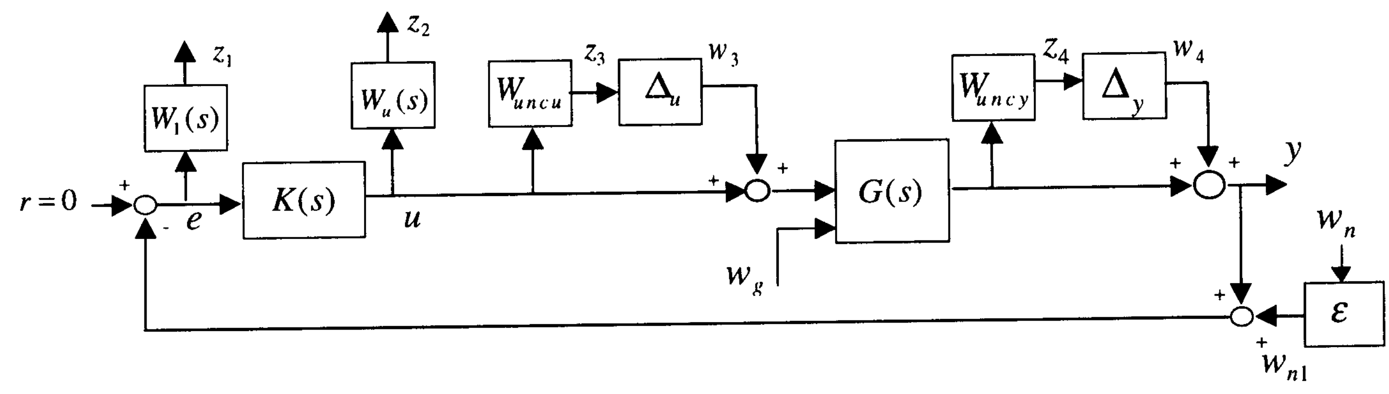

Figure 8.
Setup for robust control design.

A μ-synthesis consists of finding the optimal controller that minimizes the peak value of $\mu_\Gamma[T_{wz}(j\omega)]$ over all frequencies. That is,

$$\min_{K(s)\in S}\sup_{\omega\in\mathbb{R}}\mu_\Gamma[T_{wz}(j\omega)] \quad . \tag{23}$$

Compare this with the optimization problem for the H_∞ controller design in Equation 17. The main benefit offered by μ-synthesis is robust performance. That is, according to the Main Loop Theorem (Balas *et al.*, 1995), if a controller achieves

$$\sup_{\omega\in\mathbb{R}}\mu_\Gamma[T_{w_s z_s}(j\omega)] < 1,$$

then both stability and the performance specification $\|T_{wz}\|_\infty < 1$ hold for all $\Delta(s) \in H_\infty$, $\|\Delta\|_\infty \le 1$, $\Delta(j\omega) \in \Omega$.

It is well known that no algorithm is yet available to compute $\mu_\Gamma(M)$ in the general case (including our case). Thus, the optimization problem (Equation 23) cannot be solved directly. However, the so-called *D-K iteration* algorithm (Balas *et al.*, 1995) has been proposed to minimize an upper bound for μ_Γ. The D-K iteration is an attempt to solve

$$\min_{K\in S, D_l, D_r}\|D_l T_{w_s z_s} D_r^{-1}\|_\infty \tag{24}$$

where the so-called left and right D-scales $D_l(s)$, $D_r(s) \in H_\infty$ are minimum-phase and have frequency responses of the form:

$$D_l(j\omega)\in D_l := \{\mathrm{diag}\{d_1, d_2, d_3, I_4\} : d_1, d_2, d_3 \in \mathbb{R}_+\} \quad , \tag{25}$$

$$D_r(j\omega)\in D_r := \{\mathrm{diag}\{d_1, d_2, d_3, I_3\} : d_1, d_2, d_3 \in \mathbb{R}_+\} \quad . \tag{26}$$

This algorithm involves an iterative sequence of minimizations over $K(s) \in S$ (holding the D-scales fixed) using the H_∞ technique, then over the D-scales (holding $K(s)$ fixed).

Simulation Results

In this section, we use the Dryden model with parameters $\sigma_w = 7\ m/s$, $L_w = 580m$ to generate severe wind gusts for simulation purposes. **Figure 10** shows the gust vector used in our simulations.

Figure 11 shows a magnitude plot of the frequency response of the Dryden filter for simulation. We can see that the performance specification enforced by the weighting function should result in efficient GLA.

Time-domain simulations were conducted and results are presented below. The results confirm that the H_∞ controller can dramatically reduce the effect of wind gusts on the vertical acceleration of the aircraft for the nominal model comparing to the results of different H_2 (LQG) controllers (Botez, Boustani and Vayani, 1999), (Aouf, Boulet and Botez, 2000).

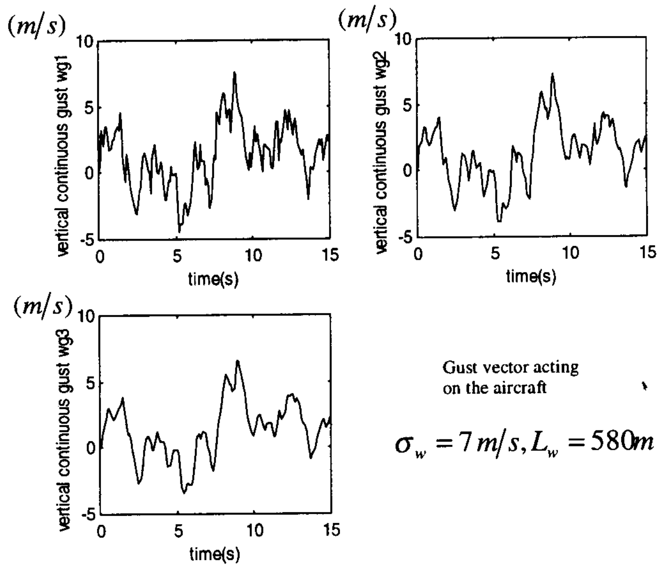

Figure 10.
Gust signals for simulation.

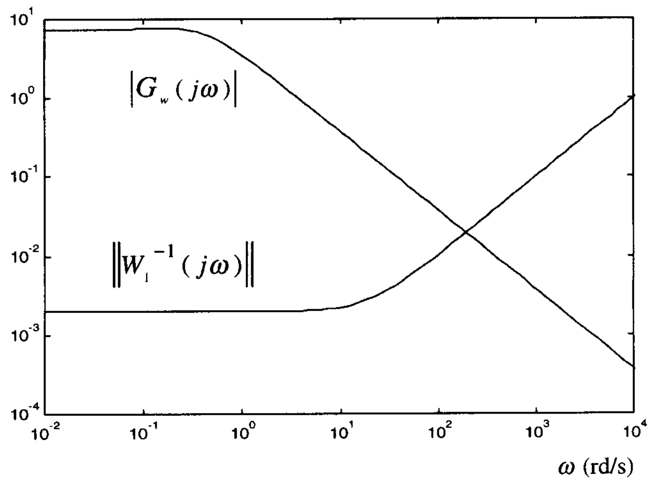

Figure 11.
Dryden filter and performance weighting.

The goal of the simulation with the nominal model (without uncertainties) is to show that our H_∞ controller can deal with strong turbulence without exciting the flexible modes or generating large control angles that would saturate the control surfaces. **Figures 12 a** and **12b** show, respectively, the effect of the gust $w_g = [w_{g1}\ w_{g2}\ w_{g3}]^T$ on the B-52 aircraft without using a feedback controller, and with the H_∞ regulator.

These plots show a dramatic improvement in flight comfort. **Figure 13** shows the control angles. Notice that the angle swings of the elevator and the horizontal canard control surfaces were reasonable. However, the rate of change of the angles seems a bit fast. With known rate limits, one could redesign the controller with lower cutoff frequencies in W_u^{1} .

Figure 14 below shows the magnitudes of the weighting functions

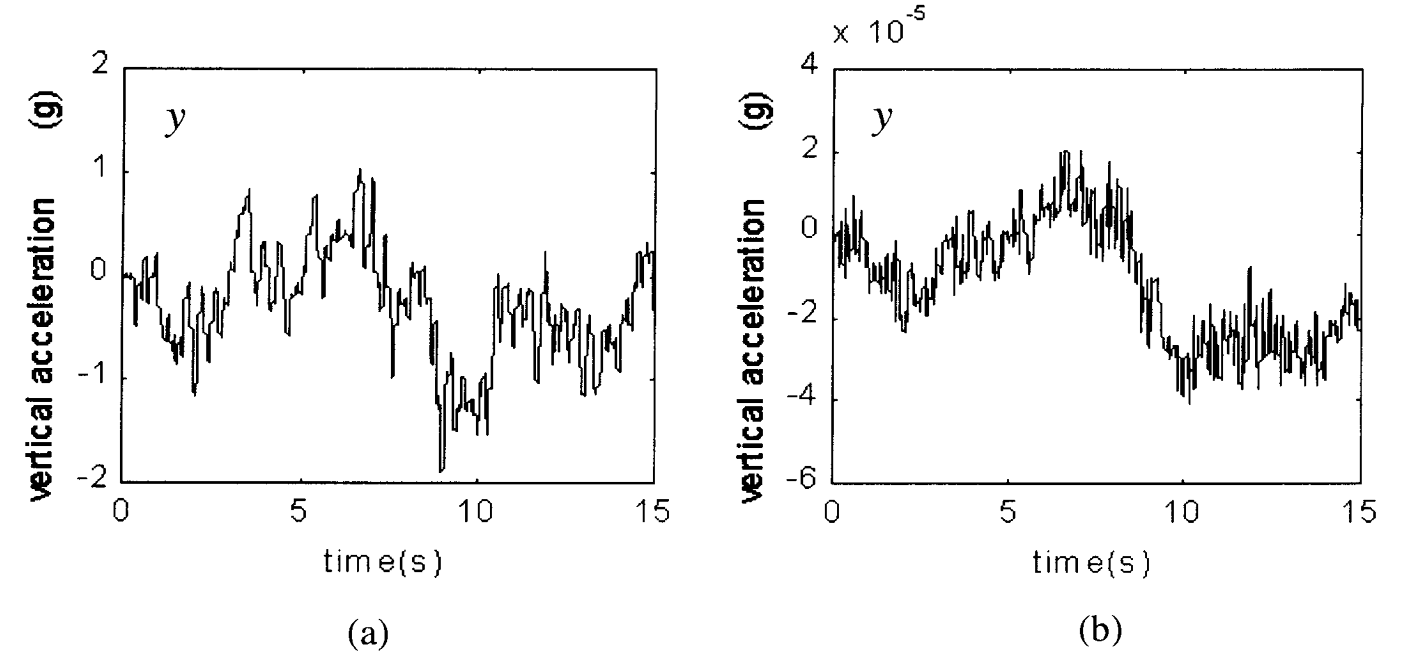

Figure 12.
(a) Open-loop response;
(b) Closed-loop response with H_∞ control.

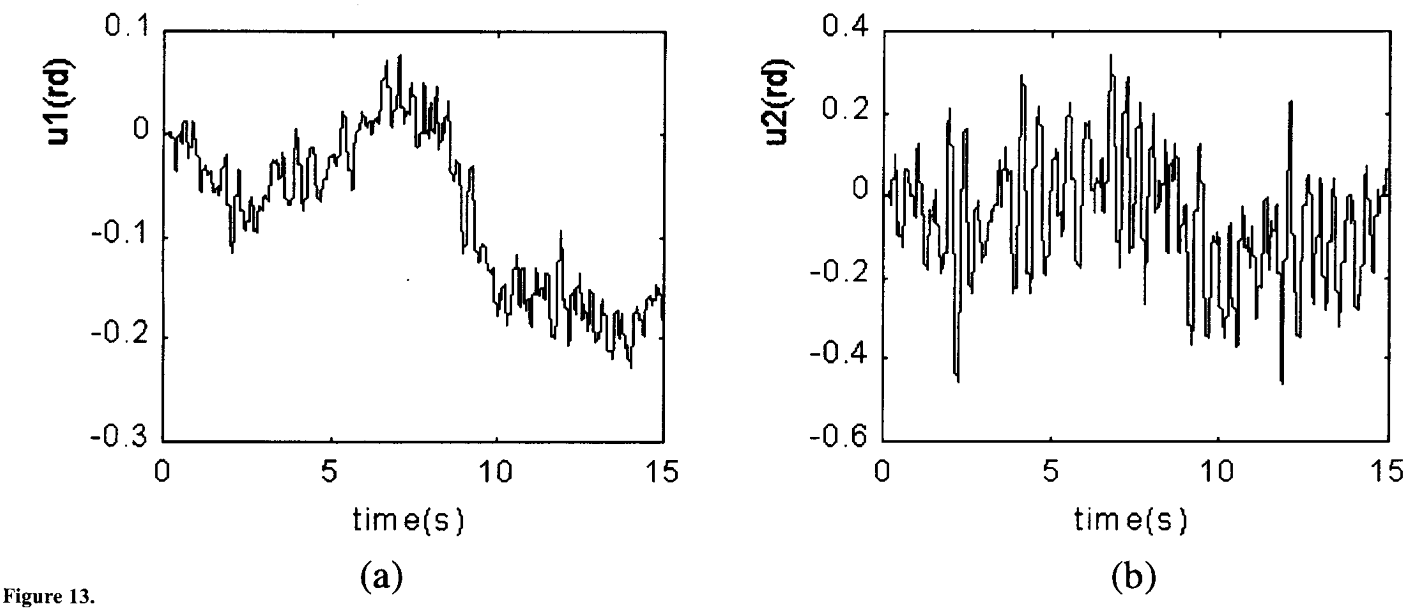

Figure 13.
(a) Elevator angle;
(b) Horizontal canard angle.

$$W_{uncu}(s) = \begin{bmatrix} W_{uncu1}(s) & 0 \\ 0 & W_{uncu2}(s) \end{bmatrix}, W_{uncy}(s)$$

in Equations 18 and 19. These weighting functions specify the amount of uncertainty in the actuators and the sensor, respectively. For the simulation, we arbitrarily specified nearly 20% of uncertainty at low frequencies for the first actuator (elevator) and around 8% of uncertainty for the second actuator (horizontal canard). For the sensor, we assumed an uncertainty of 3.5% at low frequencies. These uncertainties grow with frequency until they reach a constant level at high frequencies.

Our μ controller obtained using a D-K iteration reached the robust performance specified. **Figure 15** shows the μ-bounds for the controller obtained in the second D-K iteration. The maximum of the upper bound for μ across frequencies is equal to 0.792, and therefore robust performance was achieved.

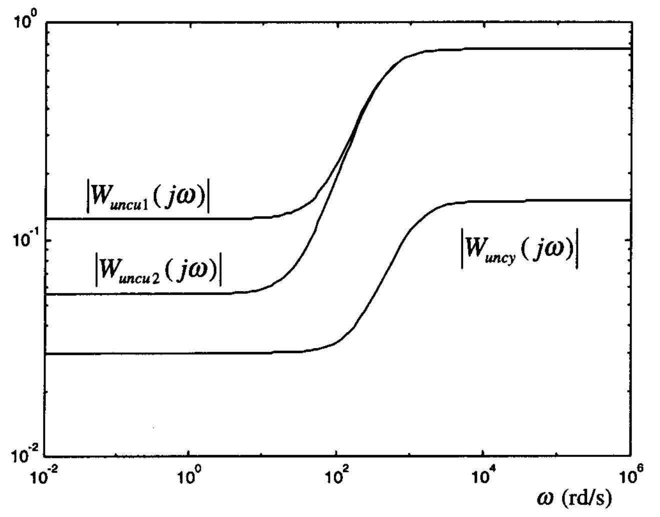

Figure 14.
Norm bounds for uncertainties.

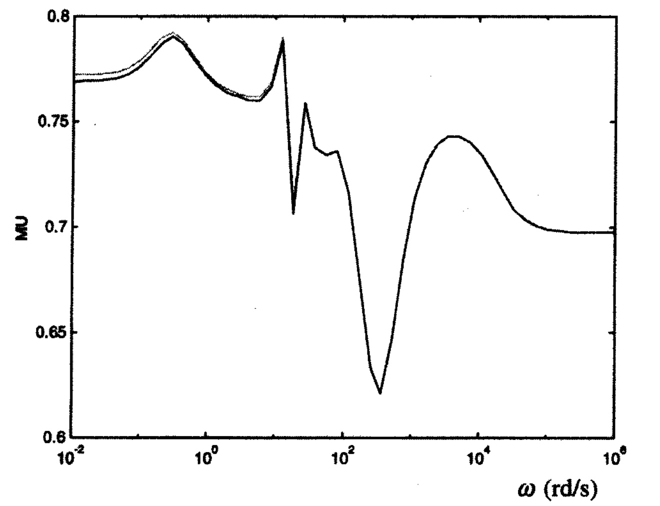

Figure 15.
Upper and lower bounds on μ_T for the μ design.

An H_∞ controller designed for the model with uncertainties led to an maximum norm of the frequency response of the closed-loop system equal to 15.35. This is too high and hence unacceptable from a robust performance point of view. A μ-analysis was performed for the H_∞ controller and the results are shown in **Figure 16**. It is seen that the maximum of μ_T obtained with the H_∞ controller is equal to 3.1. This value being much larger than one confirms the loss of robust performance.

This was expected because the H_∞ design is unable to take into account the structure of the uncertainty as opposed to the μ-design.

Conclusion

We presented a GLA H_∞ -optimal controller design for a B-52 aircraft model with flexible modes. The gust was generated with a Dryden power spectral density model. This kind of model lends itself well to frequency-domain performance

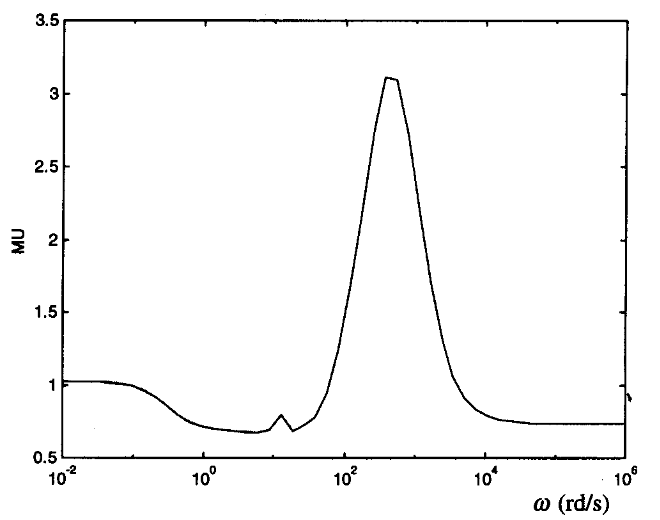

Figure 16.
Upper and lower bounds on μ_T for the H_∞ design.

specifications in the form of weighting functions. The H_∞ controller was shown to meet the desired performance specification with reasonably small control surface deflection angles. A μ design was then developed for a perturbed model including multiplicative uncertainties in the actuators and the sensor. The μ controller reached the robust performance level specified. We also compared an H_∞ controller design for this uncertain model with the μ design. We pointed out the loss of robust performance of the H_∞ design compared to the μ design. Future research will focus on the issues related to uncertain modal parameters and different flight envelopes.

References

[1] Aouf, N., Boulet, B., Botez, R. (2000). "H_2 and H_∞ Optimal Gust Load Alleviation for a Flexible Aircraft." *Proc. 2000 American Control Conference*, Chicago, June 28-30, pp. 1872-1876.

[2] Balas, G.J., Doyle, J.C., Glover, K., Packard, A., Smith, R. (1995) "μ -Analysis and Synthesis Toolbox." MUSYN Inc, and the MathWorks, Inc.

[3] Botez, R., Boustani, I. and Vayani, N. (1999). "Optimal Control Laws for Gust Load Alleviation." *Proc. 46th Annual CASI Conference*, Montréal, May 3-5, pp. 649-655.

[4] Doyle, J.C., Glover, K., Khargonekar, P., Francis, B. (1988). "State Space Solutions to Standard H_2 and H_∞ Control Problems." *IEEE Trans. Automatic Control* AC-24(8), 731-747.

[5] Mclean, D. (1978). "Gust Load Alleviation Control Systems for Aircraft." *Proc. IEE*, Vol.125, No.7, July, pp. 675-685.

[6] Mclean, D. (1990). "Automatic Flight Control Systems." Prentice Hall International, Series in Systems and Control Engineering.

[7] Niewoehner, R.J., and Kaminar, I.I. (1996). "Design of an Autoland Controller for an F-14 Aircraft Using H_∞ Synthesis." *Journal of Guidance, Control, and Dynamics*, Vol. 19, No 3, May, pp. 656-663.